A Rheological and Morphological Model for Blends of Flexible and Rigid Macromolecules

BRIAN J. EDWARDS

Department of Chemical Engineering
The University of Tennessee
Knoxville, TN 37996

KAREN L. WILLIAMS

Department of Mechanical Engineering
Vanderbilt University
Nashville, TN 37235

A model is developed that describes the complicated rheology and morphology of thermoplastic polymers blended with relatively small amounts of liquid-crystalline polymers (LCPs). Such blends typically display properties superior to, but more complicated than, those of ordinary thermoplastic polymers. Viscosity predictions are obtained with this model that exhibit the wide range of behavior that is observed experimentally in these blended materials for both shear and elongational flows. For example, the viscosity-composition curve can display a minimum at low compositions of LCP, and the addition of an LCP to a thermoplastic polymer can result in a reduction in the shear viscosity but an increase in the elongational viscosity. Corresponding morphological descriptions are also obtained for the internal microstructure of the blends that provide information about the underlying causes of the complicated rheological behavior.

INTRODUCTION

Blends of thermoplastic polymers (TPs) and liquid-crystalline polymers (LCPs) have generated some intense interest over the past decade because of several advantages they offer relative to conventional TPs or blends of these polymers (1–8). For instance, a small amount of LCP added to a thermoplastic polymer can alter the viscosity of the thermoplastic matrix phase significantly. In some processes, such as melt spinning or film blowing, a high elongational viscosity is required because of the extensional nature of the process. In other processes, such as injection molding, low shear viscosity materials are preferable in order to ensure complete mold filling and fast processing cycles (6). Experimental evidence suggests that small amounts of LCPs added to thermoplastic polymers can reduce the shear viscosity of the neat TP, and, potentially, at the same time increase its elongational viscosity, thus aiding both types of processes (6).

Some phenomenological correlations have appeared in the literature regarding these unusual blends. Valenza and La Mantia (9) demonstrated that the shear viscosities of blends of LCPs and thermoplastic polymers decrease with increasing LCP concentration and are between those of the two homopolymers when the ratio of the neat TP to LCP viscosities is much larger than unity. They also showed that the shear viscosity of the blends usually displays a minimum with LCP concentration when the viscosity ratio mentioned above is about unity.

Material properties can also be positively affected by addition of small amounts of LCPs to thermoplastic polymers. For example, Kiss (8) found that by blending polybutyleneterephthalate with an liquid-crystalline polyester, the tensile modulus of injection molded mini-bars was increased approximately 25% over that of the neat polymer. Since LCPs are generally expensive, it is also beneficial that these key property enhancements are exhibited for small LCP concentrations.

To date, no viable models for blends of thermoplastic polymers and LCPs have appeared in the literature. In this article, a model is developed and investigated for the purpose of describing the rheological behavior and the associated gross morphological characteristics of the intrinsic microstructure. It is

demonstrated that the model can exhibit behavior very similar to that which is observed experimentally, such as the minimum in the viscosity-composition curve and the higher elongational but lower shear viscosity of LCP-blended thermoplastics. Furthermore, the model allows an examination of the microstructural interactions between the LCP and thermoplastic polymer that lead to these strange rheological properties.

A MODEL FOR BLENDS OF THERMOPLASTIC AND LIQUID-CRYSTALLINE POLYMERS

Using methodology developed over the past decade, a model can be constructed for blends of thermoplastic and LC polymers. This methodology is based on the reformulation of non-equilibrium thermodynamics in terms of its underlying mathematical structure that is essentially invariant of the physical system or material under investigation. The mathematical form of this underlying structure has been determined over the past decade (10–12), and, once known, allows thermodynamically consistent derivations of the local continuum equations of motion for describing the dynamical phenomena that occur in complex materials.

The starting point of the modeling effort is the realization of the appropriate variables needed to describe the material under consideration, in this case, a TP/LCP blend. Taking the material as incompressible and isothermal, three variables are needed to describe the rheology and morphology of these blends: ($\mathbf{u}$, $\mathbf{c}$, $\mathbf{m}$). The first variable, $\mathbf{u}$, is the momentum density, defined as $\mathbf{u} = \rho\mathbf{v}$, where ρ is the mass density of the fluid and $\mathbf{v}$ is the local velocity vector field. The second variable is the conformation tensor describing the distribution of orientation and extension of the thermoplastic polymer chains in the blend. It is assigned its usual definition as the second moment of the orientational distribution function, $\psi(\mathbf{x}, \mathbf{R}, t)$ (13):

$$\mathbf{c} = \int \mathbf{R}\mathbf{R}\,\psi\, d^3 R. \tag{1}$$

In this expression, $\mathbf{R}$ is the end-to-end vector of a TP chain and $\mathbf{x}$ is the Eulerian coordinate denoting the spatial position of the chain's center of mass. According to *Eq 1*, $\mathbf{c}$ has units of length squared. The final variable, $\mathbf{m}$, describes the orientational distribution of the LCP macromolecules in the blend. Its definition is similar to *Eq 1*; however, in this case, the polymer molecules are rigid and inextensible. Hence the end-to-end vector $\mathbf{R}$ is replaced by the unit vector, $\mathbf{n}$, called the *director*, which quantifies the orientation of a given rigid molecule. Thus,

$$\mathbf{m} = \int \mathbf{n}\mathbf{n}\,\phi\, d^3 n, \tag{2}$$

where $\phi(\mathbf{x}, \mathbf{n}, t)$ is the orientational distribution function of the rigid macromolecules. By this definition, the second-rank tensor $\mathbf{m}$ is required always to have a unit trace.

Next, an expression is written for the total energy, or Hamiltonian, of the material as a function of the three variables just chosen. The simplest reasonable expression is

$$H[\mathbf{u}, \mathbf{c}, \mathbf{m}] = \int \left[\frac{1}{2\rho}\mathbf{u}\cdot\mathbf{u} + \frac{\rho\alpha}{2} K\, tr\mathbf{c} - \frac{\rho\alpha k_B T}{2} \ln det\,\mathbf{c} + \frac{\rho\nu k_B T}{4}\mathbf{m} : \mathbf{m} \right] d^3 x, \tag{3}$$

where K is the Hookean spring constant, k_B is Boltzmann's constant, T is the absolute temperature, and α, ν are elastic constants that are essentially functions of the concentrations of polymer chains and rigid molecules (14). Hence they can be thought of as parameters quantifying the concentration of elasticity within the blend components.

Two main assumptions were used to arrive at this expression. First, it was assumed that the concentration of LCP in the blend was low. From a practical perspective, these blends are viable only under this condition because of the expense of LCPs. With regard to *Eq 3*, however, this assumption allowed the free energy of the LCP component to be written as a truncated Landau/de Gennes form, rather than the full expansion (10). This is commonly called *The Maier/Saupe* Potential (15). The second assumption is that the thermoplastic polymer follows the free energy of a single Maxwell mode (10), which is generally a good approximation of the gross characteristics of viscoelastic media in the linear deformation regime. Note that there is no coupling between the two modes in the Hamiltonian; i.e., there is no mixing rule for the blend. Each component is assumed not to affect the other's energetics per se, but such a dependence could be incorporated into the Hamiltonian indirectly through specifications of appropriate concentration dependencies of α and ν. The components will interact with each other dynamically, however, as dictated by the underlying mathematical structure of the dissipation bracket.

The Hamiltonian of *Eq 3* limits the applicability of the model to be derived below. Given the mathematical form of the LCP contribution to this expression, one can interpret the domain of applicability of the model in three distinct ways. First, since the interfacial energy between the TP matrix phase and LCP droplets has been neglected from *Eq 3*, the model might be construed as being limited to low deformation flows where the interfacial energy is relatively insignificant. Second, as opposed to blends of two thermoplastic polymers where interfacial energy can be very significant, one might argue that when the dispersed phase possesses liquid-crystalline order, the interfacial energy is minor relative to the bulk free energy of the LC phase, as quantified by The Maier/Saupe Potential. Third, one can argue that the elastic constant ν is proportional to the interfacial energy, and that the term $\mathbf{m} : \mathbf{m}$ quantifies an entropic measure of average droplet surface area, thereby recovering

a model of similar spirit to the Doi/Ohta Model of TP blends (16). Regardless of which of these three views one takes, the model should possess at least some domain of applicability for describing the rheological and morphological properties of TP/LCP blends. Indeed, one could assume the second view, as outlined above, and include an additional effect in the Hamiltonian of *Eq 3* associated with the interfacial energy and another variable quantifying the amount of surface area of the droplets, as in Ref. (16). Then, both effects, LCP bulk free energy and interfacial energy, would be incorporated into the ensuing model.

The methodology used to derive the model asserts that the dynamics of an arbitrary functional of the material variables, $F[\mathbf{u}, \mathbf{c}, \mathbf{m}]$, will be governed by the global evolution equation

$$\frac{dF}{dt} = \int \left[\frac{\delta F}{\delta \mathbf{u}} \cdot \frac{\partial \mathbf{u}}{\partial t} + \frac{\delta F}{\delta \mathbf{c}} : \frac{\partial \mathbf{c}}{\partial t} + \frac{\delta F}{\delta \mathbf{m}} : \frac{\partial \mathbf{m}}{\partial t} \right] d^3x = \{F, H\} + [F, H], \quad (4)$$

where $\frac{\delta F}{\delta a}$ is the functional derivative of the arbitrary functional with respect to the variable of interest, $a = (\mathbf{u}, \mathbf{c}, \mathbf{m})$, $\{F, H\}$ is the Poisson bracket of conservative dynamics operating on the Hamiltonian of *Eq 3*, and $[F, H]$ is the dissipation bracket of non-conservative phenomena (10). The Poisson and dissipation brackets have been studied extensively in (10–12, 17, 18). The Poisson bracket can be written as the sum of three subbrackets (10),

$$\{F, H\} = \{F, H\}_u + \{F, H\}_c + \{F, H\}_m, \quad (5)$$

where

$$\{F, H\}_u = -\int \left[\frac{\delta F}{\delta u_\gamma} \nabla_\beta \left(\frac{\delta H}{\delta u_\beta} u_\gamma \right) - \frac{\delta H}{\delta u_\gamma} \nabla_\beta \left(\frac{\delta F}{\delta u_\beta} u_\gamma \right) \right] d^3x, \quad (6)$$

$$\{F, H\}_c = -\int \left[\frac{\delta F}{\delta c_{\alpha\beta}} \frac{\delta H}{\delta u_\gamma} \nabla_\gamma c_{\alpha\beta} - \frac{\delta H}{\delta c_{\alpha\beta}} \frac{\delta F}{\delta u_\gamma} \nabla_\gamma c_{\alpha\beta} \right] d^3x - \int c_{\alpha\gamma} \left[\frac{\delta H}{\delta c_{\alpha\beta}} \nabla_\gamma \left(\frac{\delta F}{\delta u_\beta} \right) - \frac{\delta F}{\delta c_{\alpha\beta}} \nabla_\gamma \left(\frac{\delta H}{\delta u_\beta} \right) \right] d^3x - \int c_{\beta\gamma} \left[\frac{\delta H}{\delta c_{\alpha\beta}} \nabla_\gamma \left(\frac{\delta F}{\delta u_\alpha} \right) - \frac{\delta F}{\delta c_{\alpha\beta}} \nabla_\gamma \left(\frac{\delta H}{\delta u_\alpha} \right) \right] d^3x, \quad (7)$$

$$\{F, H\}_m = -\int \left[\frac{\delta F}{\delta m_{\alpha\beta}} \frac{\delta H}{\delta u_\gamma} \nabla_\gamma m_{\alpha\beta} - \frac{\delta H}{\delta m_{\alpha\beta}} \frac{\delta F}{\delta u_\gamma} \nabla_\gamma m_{\alpha\beta} \right] d^3x - \int m_{\alpha\gamma} \left[\frac{\delta H}{\delta m_{\alpha\beta}} \nabla_\gamma \left(\frac{\delta F}{\delta u_\beta} \right) - \frac{\delta F}{\delta m_{\alpha\beta}} \nabla_\gamma \left(\frac{\delta H}{\delta u_\beta} \right) \right] d^3x - \int m_{\beta\gamma} \left[\frac{\delta H}{\delta m_{\alpha\beta}} \nabla_\gamma \left(\frac{\delta F}{\delta u_\alpha} \right) - \frac{\delta F}{\delta m_{\alpha\beta}} \nabla_\gamma \left(\frac{\delta H}{\delta u_\alpha} \right) \right] d^3x + 2\int m_{\alpha\beta} m_{\gamma\varepsilon} \left[\frac{\delta H}{\delta m_{\gamma\varepsilon}} \nabla_\alpha \left(\frac{\delta F}{\delta u_\beta} \right) - \frac{\delta F}{\delta m_{\gamma\varepsilon}} \nabla_\alpha \left(\frac{\delta H}{\delta u_\beta} \right) \right] d^3x. \quad (8)$$

Similarly, the dissipation bracket is written as (10, 19)

$$[F, H] = -\int \Lambda_{\alpha\beta\gamma\varepsilon} \frac{\delta F}{\delta c_{\alpha\beta}} \frac{\delta H}{\delta c_{\gamma\varepsilon}} d^3x - \int \Psi_{\alpha\beta\gamma\varepsilon} \left(\frac{\delta F}{\delta m_{\alpha\beta}} - \delta_{\alpha\beta} m_{\eta\varsigma} \frac{\delta F}{\delta m_{\eta\varsigma}} \right) \left(\frac{\delta H}{\delta m_{\gamma\varepsilon}} - \delta_{\gamma\varepsilon} m_{\rho\theta} \frac{\delta H}{\delta m_{\rho\theta}} \right) d^3x - \int \Xi_{\alpha\beta\gamma\varepsilon} \left[\frac{\delta F}{\delta c_{\alpha\beta}} \left(\frac{\delta H}{\delta m_{\gamma\varepsilon}} - \delta_{\gamma\varepsilon} m_{\rho\theta} \frac{\delta H}{\delta m_{\rho\theta}} \right) + \frac{\delta H}{\delta c_{\alpha\beta}} \left(\frac{\delta F}{\delta m_{\gamma\varepsilon}} - \delta_{\gamma\varepsilon} m_{\rho\theta} \frac{\delta F}{\delta m_{\rho\theta}} \right) \right] d^3x. \quad (9)$$

In these expressions, Λ, Ψ, and Ξ are phenomenological coefficient matrices (10), to be defined shortly.

In view of the global evolution expression of *Eq 4*, local evolution equations for the material variables can be derived as

$$\rho \frac{\partial v_\alpha}{\partial t} = -\rho v_\beta \nabla_\beta v_\alpha - \nabla_\alpha p + \nabla_\beta \sigma_{\alpha\beta}, \quad (10)$$

$$\frac{\partial c_{\alpha\beta}}{\partial t} = -v_\gamma \nabla_\gamma c_{\alpha\beta} + c_{\gamma\alpha} \nabla_\gamma v_\beta + c_{\gamma\beta} \nabla_\gamma v_\alpha - \Lambda_{\alpha\beta\gamma\varepsilon} \frac{\delta H}{\delta c_{\gamma\varepsilon}} - \Xi_{\alpha\beta\gamma\varepsilon} \frac{\delta H}{\delta m_{\gamma\varepsilon}} + \Xi_{\alpha\beta\gamma\gamma} m_{\rho\theta} \frac{\delta H}{\delta m_{\rho\theta}}, \quad (11)$$

$$\frac{\partial m_{\alpha\beta}}{\partial t} = -v_\gamma \nabla_\gamma m_{\alpha\beta} + m_{\gamma\alpha} \nabla_\gamma v_\beta + m_{\gamma\beta} \nabla_\gamma v_\alpha - 2 m_{\alpha\beta} m_{\gamma\varepsilon} \nabla_\gamma v_\varepsilon - \Psi_{\alpha\beta\gamma\varepsilon} \frac{\delta H}{\delta m_{\gamma\varepsilon}} + \Psi_{\alpha\beta\gamma\gamma} m_{\rho\theta} \frac{\delta H}{\delta m_{\rho\theta}} + \Psi_{\eta\eta\gamma\varepsilon} m_{\alpha\beta} \frac{\delta H}{\delta m_{\gamma\varepsilon}} - \Psi_{\eta\eta\gamma\gamma} m_{\alpha\beta} m_{\rho\theta} \frac{\delta H}{\delta m_{\rho\theta}} - \Xi_{\gamma\varepsilon\alpha\beta} \frac{\delta H}{\delta c_{\gamma\varepsilon}} + \Xi_{\gamma\varepsilon\eta\eta} m_{\alpha\beta} \frac{\delta H}{\delta c_{\gamma\varepsilon}}, \quad (12)$$

where

$$\sigma_{\alpha\beta} = 2 c_{\gamma\beta} \frac{\delta H}{\delta c_{\alpha\gamma}} + 2 m_{\gamma\beta} \frac{\delta H}{\delta m_{\alpha\gamma}} - 2 m_{\alpha\beta} m_{\gamma\varepsilon} \frac{\delta H}{\delta m_{\gamma\varepsilon}}, \quad (13)$$

and $\frac{\delta H}{\delta \mathbf{u}} = \frac{\mathbf{u}}{\rho} = \mathbf{v}$ (10, 20). These are the general evolution equations for the TP/LCP blends that are valid regardless of the specific choice of the Hamiltonian and phenomenological coefficient matrices.

To proceed further, it is necessary to specify the Hamiltonian as *Eq 3* and the phenomenological coefficient matrices as

$$\Lambda_{\alpha\beta\gamma\varepsilon} = \frac{1}{2\lambda K \rho \alpha} (c_{\alpha\gamma}\delta_{\beta\varepsilon} + c_{\alpha\varepsilon}\delta_{\beta\gamma} + c_{\beta\gamma}\delta_{\alpha\varepsilon} + c_{\beta\varepsilon}\delta_{\alpha\gamma}), \quad (14)$$

$$\Psi_{\alpha\beta\gamma\varepsilon} = \frac{1}{\rho \upsilon k_B T \gamma} (\delta_{\alpha\gamma}\delta_{\beta\varepsilon} + \delta_{\alpha\varepsilon}\delta_{\beta\gamma}), \quad (15)$$

$$\Xi_{\alpha\beta\gamma\varepsilon} = \frac{1}{\rho k_B T} \frac{\theta}{\sqrt{\alpha \nu \lambda \gamma}} (c_{\alpha\gamma} m_{\beta\varepsilon} + c_{\alpha\varepsilon} m_{\beta\gamma} + c_{\beta\gamma} m_{\alpha\varepsilon} + c_{\beta\varepsilon} m_{\alpha\gamma}), \quad (16)$$

in which θ is a phenomenological coupling parameter that quantifies the degree of interactions between the

two polymers, λ is a characteristic relaxation time of the thermoplastic polymer, and γ is the same for the LCP. The choices of these phenomenological coefficient matrices are motivated by the simplest forms, which are consistent with the methodology of Ref. (10). The coupling parameter, θ, has been investigated for thermoplastic polymers viewed as possessing two coupled Maxwell modes of conformational rearrangements (21). Experience from that case indicates that θ should be a small, positive fraction, say in the range of $0 \leq \theta \leq 1$. When the two conformation modes are identical, $\theta = 0$, and the model reduces to the usual Upper-Convected Maxwell model in terms of a single relaxation time, $\lambda = \gamma$. Thermodynamic admissibility criteria have been established for placing bounds on θ (21), but these are not particularly useful in practice because they turn out to be flow-field dependent. In the following, past experience is used to place θ in the range indicated above.

According to *Eq 3*, the remaining functional derivatives of the Hamiltonian are (10, 20)

$$\frac{\delta H}{\delta c_{\alpha\beta}} = \frac{\rho\alpha K}{2}\delta_{\alpha\beta} - \frac{\rho\alpha k_B T}{2} c^{-1}_{\alpha\beta}, \tag{17}$$

$$\frac{\delta H}{\delta m_{\alpha\beta}} = \frac{\rho\nu k_B T}{2} m_{\alpha\beta}. \tag{18}$$

Substituting *Eqs 14–18* into the evolution equations of *Eqs 10–13* results in the material specific evolution equations investigated in the remainder of this article,

$$\frac{\partial c_{\alpha\beta}}{\partial t} = -\nu_\gamma \nabla_\gamma c_{\alpha\beta} + c_{\gamma\alpha}\nabla_\gamma \nu_\beta + c_{\gamma\beta}\nabla_\gamma \nu_\alpha - \frac{1}{\lambda} c_{\alpha\beta} + \frac{k_B T}{\lambda K}\delta_{\alpha\beta} - \frac{\nu\theta}{\sqrt{\alpha\nu\lambda\gamma}} m_{\gamma\varepsilon}(c_{\alpha\gamma} m_{\beta\varepsilon} + c_{\beta\gamma} m_{\alpha\varepsilon}) + \frac{\nu\theta}{\sqrt{\alpha\nu\lambda\gamma}} m_{\rho\theta} m_{\rho\theta}(c_{\alpha\gamma} m_{\beta\gamma} + c_{\beta\gamma} m_{\alpha\gamma}), \tag{19}$$

$$\frac{\partial m_{\alpha\beta}}{\partial t} = -\nu_\gamma \nabla_\gamma m_{\alpha\beta} + m_{\gamma\alpha}\nabla_\gamma \nu_\beta + m_{\gamma\beta}\nabla_\gamma \nu_\alpha - 2 m_{\alpha\beta} m_{\gamma\varepsilon} \nabla_\gamma \nu_\varepsilon + \frac{1}{\gamma}\delta_{\alpha\beta} m_{\rho\theta} m_{\rho\theta} - \frac{3}{\gamma} m_{\alpha\beta} m_{\rho\theta} m_{\rho\theta} - \frac{\alpha K}{k_B T}\frac{\theta}{\sqrt{\alpha\nu\lambda\gamma}} (c_{\alpha\gamma} m_{\beta\gamma} + c_{\beta\gamma} m_{\alpha\gamma}) + \frac{2\alpha K}{k_B T}\frac{\theta}{\sqrt{\alpha\nu\lambda\gamma}} m_{\alpha\beta} c_{\eta\gamma} m_{\eta\gamma}, \tag{20}$$

and *Eq 10*, in which

$$\sigma_{\alpha\beta} = \rho\alpha K c_{\alpha\beta} - \rho\alpha k_B T\delta_{\alpha\beta} + \rho\nu k_B T m_{\gamma\beta} m_{\gamma\alpha} - \rho\nu k_B T m_{\alpha\beta} m_{\gamma\varepsilon} m_{\gamma\varepsilon}. \tag{21}$$

In the next section, these equations will be solved for steady-state shear and elongational flow to determine the rheological properties of sample blends and the associated morphological characteristics of the fluids.

SAMPLE CALCULATIONS OF THE RHEOLOGY OF TP/LCP BLENDS

In order to investigate the rheological and morphological characteristics of the model introduced in the previous section, a homogeneous flow field is assumed, so that only *Eqs 19* and *20* need to be solved simultaneously for the components of **c** and **m** for a given deformation rate. Subsequently, the extra stress in the fluid can be determined according to *Eq 21*. Two flow fields are examined herein: steady shear and steady uniaxial elongational flow. In the former case, the only non-zero component of the velocity gradient tensor is the shear rate, $\dot{\gamma}$, and in the latter, the non-zero components are the diagonal elements, which are proportional to the elongation rate.

For computational convenience, the evolution equations (*Eqs 19* and *20*), as well as the extra stress tensor expression, *Eq 21*, are made dimensionless according to the following assignations: $\tilde{c}_{\alpha\beta} = Kc_{\alpha\beta}/k_B T$, $\tilde{\sigma}_{\alpha\beta} = \sigma_{\alpha\beta}/\rho k_B T\sqrt{\alpha\nu}$, $\tilde{t} = t/\sqrt{\lambda\gamma}$, and $\tilde{\nabla}_\gamma \tilde{\nu}_\varepsilon = \sqrt{\lambda\gamma}\,\nabla_\gamma \nu_\varepsilon$. With these definitions, the equations of motion and the extra stress tensor expression can be recast in dimensionless form in terms of only three parameters: the ratio $R = \alpha/\nu$ that effectively quantifies the concentration of rigid molecules in the blend, the ratio $V = \gamma/\lambda$ that effectively quantifies the relative viscosities of the pure LCP and TP components of the blend, and the coupling parameter, θ. For large values of R, the blend is almost pure thermoplastic polymer, but as this ratio decreases, the LCP component has an increased significance on the dynamics of the blends. Likewise, when the ratio V is large, the viscosity of the neat TP is much smaller than that of the LCP, and vice versa.

Numerical calculations for steady shear and elongational flow were performed using Newton's Method for solving a set of non-linear algebraic equations to within an error tolerance of 10^{-10}. Results of these calculations are presented in the following figures.

Only a few experimental programs have attempted to characterize the rheological properties of TP/LCP blends (1–9). Consequently, not enough data is available to make quantitative data fitting meaningful at present. However, certain trends in the experimental data can be identified and compared with theory to see if such a simple model has potential to describe the rheological and morphological properties of such complicated blends.

In *Fig. 1*, the dimensionless zero shear-rate viscosity, η^0_s, is plotted versus $1/R$ for parameter values $V = 1$ and $\theta = 1/2$. This corresponds to a blend in which the viscosities of the neat thermoplastic and LC polymers are equivalent, and to a moderate degree of coupling between the two components. Since the concentration of LCP in the blend varies inversely with R, moving along the abscissa from left to right corresponds to increasing the LCP concentration of the blend. As evident from the figure, for reasonable values of the parameters, η^0_s displays a minimum as a function of the blend composition. Such behavior has been observed repeatedly in experiments (3, 5, 6, 9). Furthermore, this viscosity variation can range over several orders of magnitude, as also found experimentally. Note also that as $1/R \to 0$, the blend becomes a

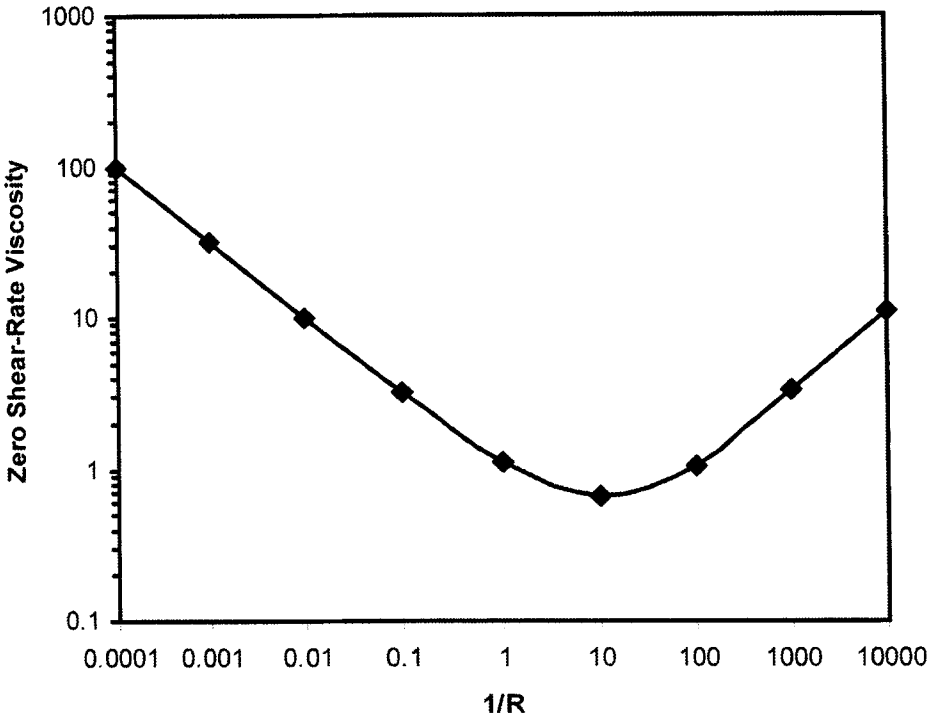

Fig. 1. Dimensionless zero shear-rate viscosity, η_s^0, versus the concentration ratio, $1/R$, for parameter values $V = 1$ and $\theta = 1/2$.

pure TP, thus providing a relative gauge of its viscosity. It is thus evident that at low LCP concentrations, the viscosity of the blend is lower than that of the pure TP, and only at relatively high concentrations of LCP can the blend manifest a higher viscosity than the pure TP.

In this model, θ defines the degree of coupling between the thermoplastic and liquid-crystalline polymer phases. In *Fig. 1*, this parameter is arbitrarily set to 1/2, this value being in the exact middle of what is considered to be the acceptable range, $0 \leq \theta \leq 1$. As θ decreases, the coupling between the two phases lessens, and the minimum in the viscosity-composition curve abates. As θ increases beyond 1/2, the minimum becomes deeper, indicating a greater degree of improvement in the shear properties of the blend.

Figure 2 displays the corresponding plot for the dimensionless zero shear-rate, first normal-stress coefficient, Ψ_1^0, versus $1/R$ for the same parameter values as *Fig. 1*. Although no experimental data is available for comparison, the model predictions for this rheological characteristic function indicate a behavior qualitatively similar to that of the shear viscosity: a minimum occurs in the coefficient versus composition curve, and the coefficient for the blends is always lower than that of the pure TP, at least at low to moderate concentrations. Furthermore, this coefficient is always roughly twice the magnitude of the zero shear rate viscosity.

Figure 3 displays the model predictions for η_s^0 versus composition $(1/R)$ for parameter values $V = [0.1, 0.01]$ and $\theta = 1/2$. These cases correspond physically to blends of thermoplastic and LC polymers where the viscosity of the pure TP is significantly larger than that of the pure LCP. Experimentally, it has been observed that these blends typically display viscosities that are between those of the pure TP and LCP, and decrease with increasing LCP concentration (9). As evident in the figure, the viscosities of the blends decrease consistently with increasing LCP concentration, as expected experimentally, with a small plateau region appearing at intermediate concentrations. Such a plateau region has been observed for several TP/LCP blends—see *Fig. 1* of (9). Also, as the viscosity of the LCP decreases relative to that of the TP, i.e., as V decreases, the viscosities of the blends increase at low compositions, but appear to saturate at high concentrations of LCP.

In *Fig. 4*, the dimensionless zero elongation-rate viscosity, η_e^0, is plotted versus LCP composition $(1/R)$ for uniaxial elongational flow using the same parameter values as in *Figs. 1* and *2*. As evident, η_e^0 displays the same qualitative behavior with LCP composition as η_s^0: there is a significant minimum at intermediate compositions, mirroring the behavior of *Figs. 1* and *2*. Consequently, it does appear that the model can capture the experimentally observed behavior that the LCP can both decrease and increase the elongational viscosity of the pure TP (6, 7). However, the model suggests that both increasing the elongational viscosity of the TP and simultaneously decreasing its shear viscosity is not feasible at vanishingly small deformation rates. This can, however, still be achieved at finite, reasonable values of the shear and elongation

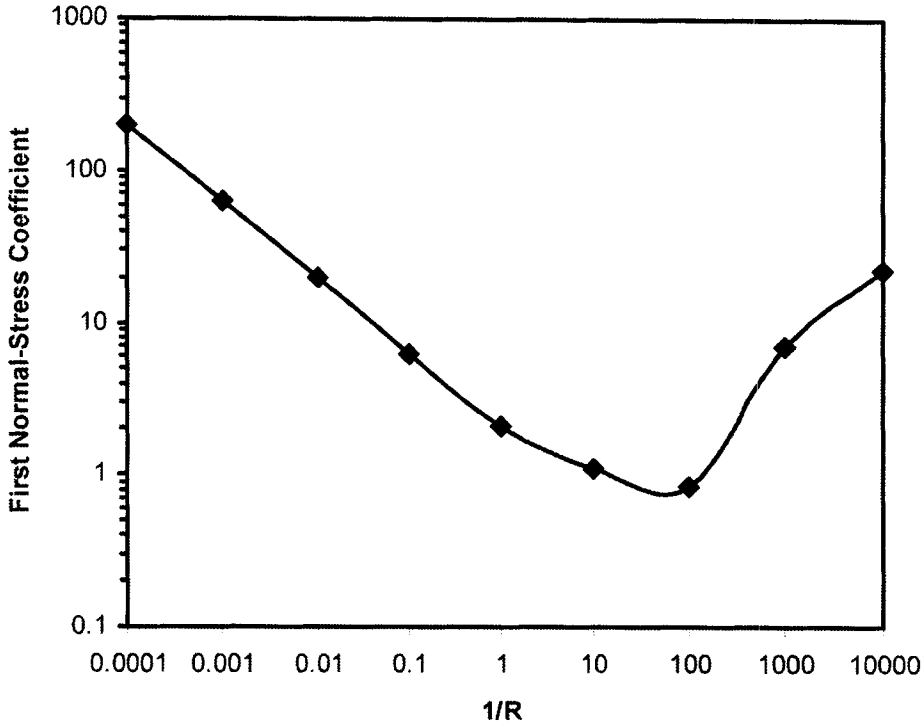

Fig. 2. Dimensionless zero shear-rate, first normal-stress coefficient, Ψ_1^0, versus the concentration ratio, 1/R, for parameter values V = 1 and θ = 1/2.

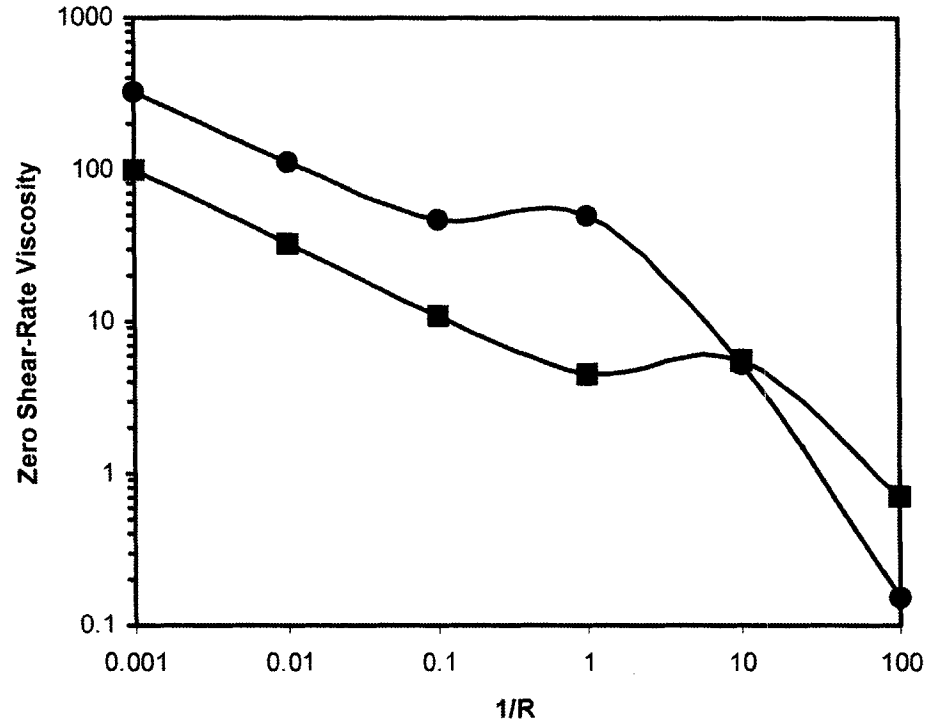

Fig. 3. Dimensionless zero shear-rate viscosity, η_s^0, versus LCP composition (1/R) for parameter values V = 0.1 (filled squares), V = 0.01 (filled circles), and θ = 1/2.

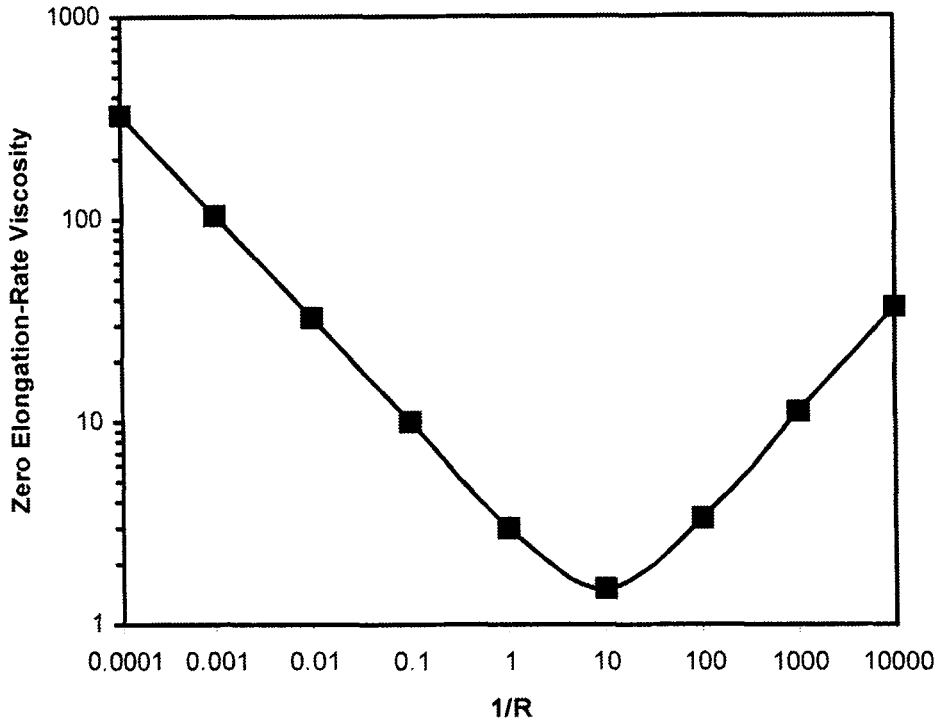

Fig. 4. The dimensionless zero elongation-rate viscosity, η_e^0, versus LCP composition (1/R) for uniaxial elongational flow for parameter values V = 1 and θ = 1/2.

rates, outside of the Newtonian region at very low deformation rates. At intermediate deformation rates, the shear viscosity can display severe shear thinning and the elongational viscosity can display a thickening behavior (7). As shown below, both of these behaviors are described by the model.

In *Fig. 5*, the shear viscosity is plotted versus shear rate for $V = 1$, $\theta = 1/2$, and several values of R. For high values of R, where the blend is mostly composed of the TP, the viscosity is Newtonian. This is to be expected since as $R \to \infty$ the material is purely thermoplastic, and this component has been modeled in the preceding section as an Upper-Convected Maxwell Mode, which displays always a constant viscosity. Of course, most neat thermoplastic polymers manifest shear-thinning behavior, but in the limit of small shear rates, they display constant Newtonian viscosities. It would be very easy to incorporate a more complicated model for the TP component into the model presented herein, along the lines discussed in Ref. (10), that does allow for a shear-thinning viscosity of the neat TP at intermediate and high shear rates. However, this is not done at present so that the core behavior of the model can be examined under the simplest set of circumstances; i.e., without distracting from the main features of the model. As $R \to 0$, the model does predict shear-thinning behavior, as caused by the interactions between the two blend components at increasing LCP concentration. Furthermore, as LCP concentration increases, the degree of shear thinning intensifies, as noticed in some experiments (3, 6).

In *Fig. 6*, the elongational viscosity is plotted versus stretch rate for $V = 1$, $\theta = 1/2$, and several values of R. At low concentrations of LCP, one observes the usual behavior of a neat TP: a constant viscosity at low stretch rates, obeying the Trouton formula, followed by an increase in the viscosity at higher elongation rates. Such behavior has been observed experimentally for many neat TPs, as well as some TP/LCP blends (7). Once the blend contains a significant LCP component, the elongational viscosity can actually decrease with increasing stretch rate, as has also been observed experimentally (2, 7). As in the experiments of Ref. (7), the model switches from thickening to thinning behavior as the concentration of the LCP increases.

The model can also give indications as to the microstructural nature of the rheological behavior thus far observed. In *Fig. 7*, the primary eigenvalues of the second-rank tensors **c** and **m** are plotted versus dimensionless shear rate for $V = 1$, $\theta = 1/2$, and two values of R. These eigenvalues give an impression as to the extension from the quiescent spherical orientational distribution of the microstructural components. At vanishingly small shear rates, the tensor **c** should possess unit eigenvalues, and the tensor **m** should have eigenvalues equal to one third; thus both indicate random distributions of orientation. As the shear rate increases, it is evident from the figure that the microstructural elements composing the TP component of the blend deform vigorously with the magnitude of the flow field, as is expected. Furthermore, the

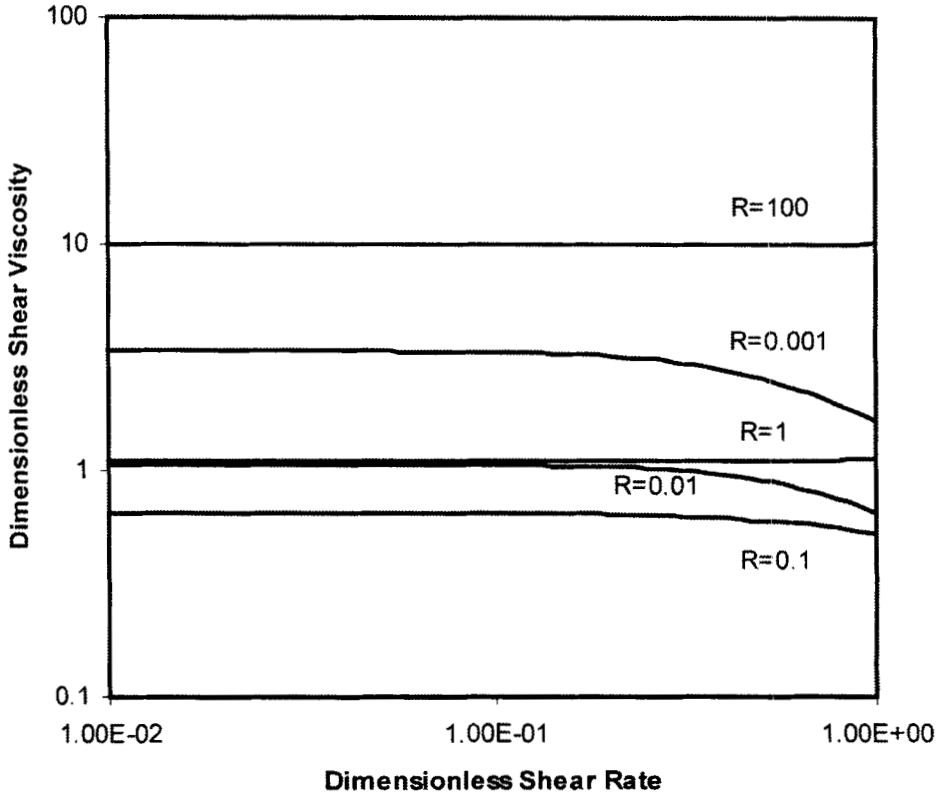

Fig. 5. The dimensionless shear viscosity versus dimensionless shear rate for $V = 1$, $\theta = 1/2$, and R values as indicated on the plot.

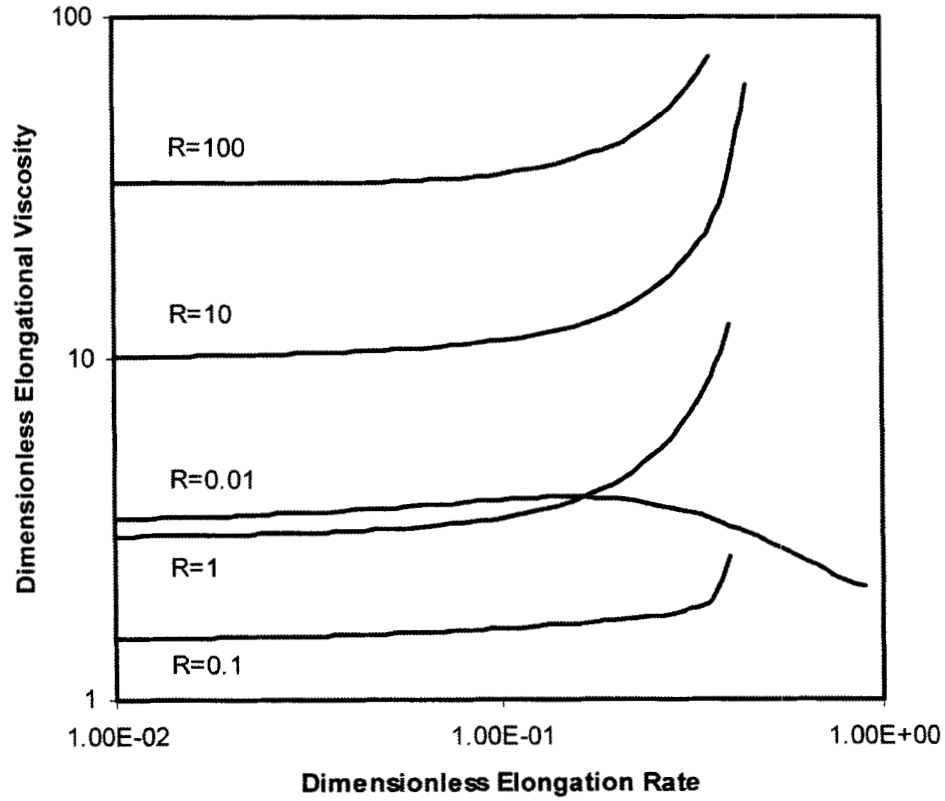

Fig. 6. The dimensionless elongational viscosity versus dimensionless stretch rate for $V = 1$, $\theta = 1/2$, and R values as indicated on the plot.

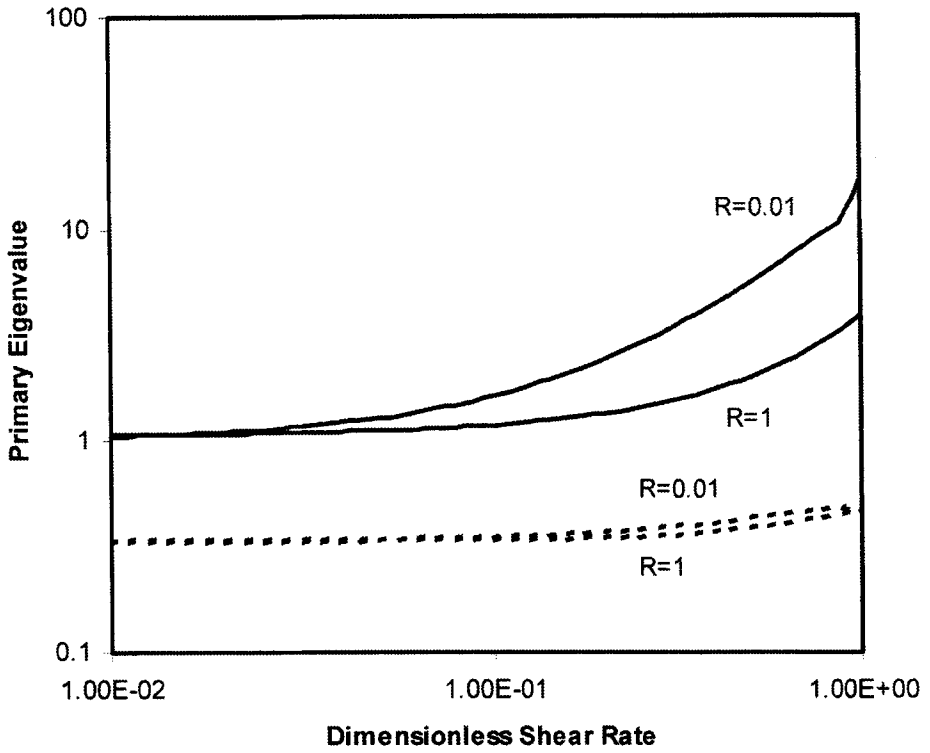

Fig. 7. The primary eigenvalues of the second-rank tensors **c** *and* **m** *versus dimensionless shear rate for* $V = 1$, $\theta = 1/2$, *and* R *values as indicated on the plot. The solid lines represent the eigenvalues of* **c**, *and the dashed lines represent the eigenvalues of* **m**.

LCP component does not experience much in the way of deformation, although it is oriented to a fair degree by the imposed shear field. The interesting feature of the model, however, is that the presence of the LCP actually induces more deformation of the TP component, thus leading to the shear-thinning behavior noticed in *Fig. 5*. Consequently, the model seems to predict that the increased degree of shear thinning with increased LCP component concentration is due to the augmentation it provides to the deformation of the TP component.

In *Fig. 8*, the primary eigenvalues of the second-rank tensors **c** and **m** are plotted versus dimensionless stretch rate for $V = 1$, $\theta = 1/2$, and the same two values of R as in *Fig. 7*. Again, the magnitude of the flow field has a greater effect on the deformation of the TP component of the blend. Note, however, that in this type of flow, the LCP component reduces the intensity of the deformation, rather than augmenting it as in shear flow. This reduction in deformation, at a given stretch rate, is probably then associated with the presence of the elongational thickening or thinning behavior observed in *Fig. 6*. Thus it seems that the effect of the LCP component has upon the rheological properties of the blend depends greatly on the type of flow field that is applied to these materials.

CONCLUSIONS

In this article, a model was developed to describe the complicated rheology and morphology of thermoplastic polymers blended with relatively small amounts of liquid-crystalline polymers. Viscosity predictions were obtained with this model that exhibited the wide range of qualitative behavior that is observed experimentally in these blended materials for both shear and elongational flows. Viscosity-composition curves displayed minima at low compositions of LCP, for both shear and elongational flow fields. In elongational flow fields, both a thickening and a thinning behavior with increasing stretch rate was observed, depending on the relative concentration of the LCP component. The corresponding morphological implications were also considered through the model, thus providing information about the internal microstructural states that give rise to the complicated rheological behavior.

ACKNOWLEDGMENTS

This material is based upon work supported by the National Science Foundation through grant number EEC-9820489. Any opinions, findings, conclusions, or recommendations expressed in this material are those of the authors and do not necessarily reflect the views of the National Science Foundation.

REFERENCES

1. F. P. La Mantia, A. Valenza, and F. Scargiali, *Polym. Eng. Sci.*, **34**, 799 (1994).
2. D. Beery, S. Kenig, A. Siegmann, and M. Narkis, *Polym. Eng. Sci.*, **32**, 14 (1992).
3. F. P. La Mantia, A. Valenza, M. Paci, and P. L. Magagnini, *Rheo. Acta*, **28**, 417 (1989).

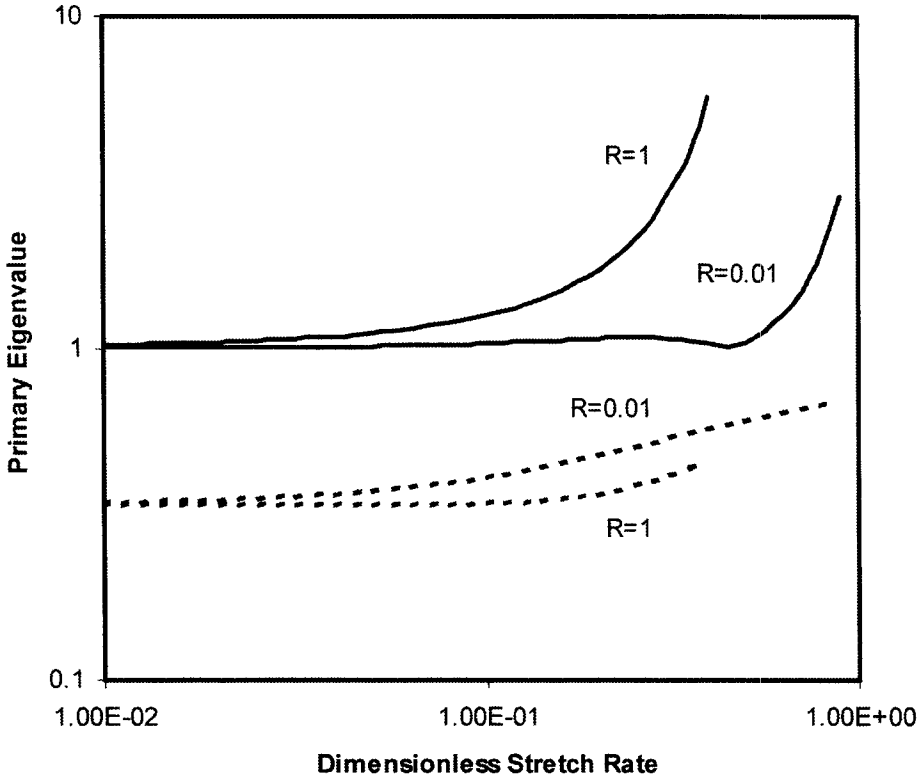

Fig. 8. The primary eigenvalues of the second-rank tensors **c** *and* **m** *versus dimensionless stretch rate for* $V = 1$, $\theta = 1/2$, *and R values as indicated on the plot. The solid lines represent the eigenvalues of* **c**, *and the dashed lines represent the eigenvalues of* **m**.

4. Y. Yongcheng, F. P. La Mantia, A. Valenza, V. Citta, U. Pedretti, and A. Roggero, *Europ. Polym. J.*, **27**, 723 (1991).
5. F. P. La Mantia, A. Valenza, M. Paci, and P. L. Magagnini, *Polym. Eng. Sci.*, **30**, 7 (1990).
6. F. P. La Mantia, A. Valenza, and P. L. Magagnini, *J. Appl. Polym. Sci.*, **44**, 1257 (1992).
7. F. P. La Mantia, M. Paci, and P. L. Magagnini, *Rheo. Acta*, **36**, 152 (1997).
8. G. Kiss, *Polym. Eng. Sci.*, **27**, 410 (1987).
9. A. Valenza and F. P. La Mantia, *Polym. Networks Blends*, **3**, 125 (1993).
10. A. N. Beris and B. J. Edwards, *Thermodynamics of Flowing Systems*, Oxford University Press, New York (1994).
11. M. Grmela and H. C. Öttinger, *Phys. Rev. E*, **56**, 6620 (1997).
12. H. C. Öttinger and M. Grmela, *Phys. Rev. E*, **56**, 6633 (1997).
13. R. B. Bird, C. F. Curtiss, R. C. Armstrong, and O. Hassager, *Dynamics of Polymeric Fluids, Vol. 2, 2nd Ed.*, John Wiley and Sons, New York (1987).
14. M. Dressler, B. J. Edwards, and H. C. Öttinger, *Rheol. Acta*, **38**, 117 (1999).
15. W. von Maier and A. Saupe, *Z. Naturforschg.*, **13a**, 564 (1958).
16. M. Doi and T. Ohta, *J. Chem. Phys.*, **95**, 1242 (1991).
17. B. J. Edwards, *J. Non-Equilib. Thermodyn.*, **23**, 301 (1998).
18. B. J. Edwards, A. N. Beris, and H. C. Öttinger, *J. Non-Equilib. Thermodyn.*, **23**, 334 (1998).
19. B. J. Edwards, M. Dressler, M. Grmela, and A. Ait-Kadi, *Rheol. Acta*, **42**, 64 (2003).
20. A. N. Beris and B. J. Edwards, *J. Rheol.*, **34**, 55 (1990).
21. B. J. Edwards, A. N. Beris, and V. G. Mavrantzas, *J. Rheol.*, **40**, 917 (1996).